THE JOURNAL OF PHYSICAL CHEMISTRY B

ARTICLE

pubs.acs.org/JPCB

Dynamics of Ion Transfer Potentials at Liquid−Liquid Interfaces: The Case of Multiple Species

Konstantin Zhurov, Edmund J. F. Dickinson, and Richard G. Compton*

Department of Chemistry, Physical and Theoretical Chemistry Laboratory, Oxford University, South Parks Road, Oxford, United Kingdom OX1 3QZ

Supporting Information

ABSTRACT: The dynamic evolution of a water−nitrobenzene system with both solvents containing an initially equimolar mixture of two monovalent binary electrolytes, sharing a common cation, is simulated using the Nernst−Planck−Poisson finite difference method. The effect of single ion partition coefficients and diffusion coefficients on the evolution of potential across the liquid−liquid interface is investigated. Two separable components of the potential difference are observed: a static component localized at the liquid−liquid interface and a diffuse component with dynamic spatial expansion. The former is shown through novel calculations to be dependent on an apparent partition coefficient of the system, defined to be dependent on the partition coefficients of the two constituent salts such that the static component also depends on the single ion partition coefficient of the shared cation. The dynamic component depends on the same apparent partition coefficient; further, its dependence on the diffusion coefficients of the constituent ions is investigated, and the time scales of the potential difference formation are revealed. The evolution of the system can be described in three stages with short time behavior dominated by partition of ions and long-time behavior dominated by recovery of electroneutrality. The dynamics were correlated to those recently discussed for a simpler system [Zhurov, K. et al. *J. Phys. Chem. B*, **2011**, *115*, 6909−6921].

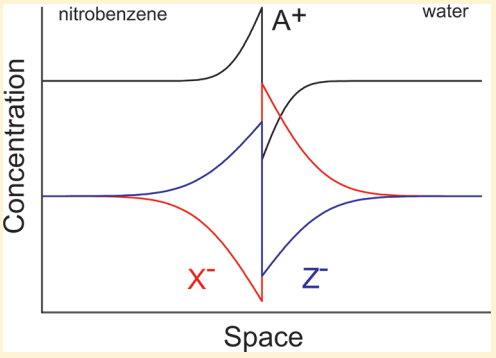

1. INTRODUCTION: THE INTERFACE BETWEEN TWO IMMISCIBLE ELECTROLYTE SOLUTIONS (ITIES)

1.1. General Understanding of ITIES. An ITIES is an interface between two immiscible electrolyte solutions. It is a type of liquid−liquid interface that arises when two immiscible solutions containing dissolved electrolytes are brought into contact. Typically, ion transfer reactions take place across the ITIES as the interface equilibrates. These arise from ionic species partitioning into one particular solvent for better energetic stabilization, which gives rise to concentration gradients and hence diffusion. Given different diffusion coefficients for different ions, the ions will diffuse at different rates, causing charge separation and hence a potential difference.

ITIES have been the subject of considerable experimental and theoretical interest for several decades, as they have applications in numerous fields including biochemistry, microscopy, and extraction chemistry.[1−6] Recent work[7] has considered dynamic aspects of the characteristic potential differences of ITIES for a simple two-species system. The current work applies and extends the methodology and theory developed in the previous work to a more complex system—that of two binary electrolytes with a common shared ion partitioning across the ITIES—thereby addressing for the first time the dynamic evolution, from initial conditions to steady state, of a two-solvent system with multiple ions, and also addressing the effect of diffusion coefficients on the dynamic evolution of the system. Previous work on such systems has tended to ignore dynamic effects.[1,8−12] These are significant, as we will show that they predict the formation of a diffuse component of the potential difference, which is transient in nature and thus not observable at equilibrium or steady state. By considering dynamic effects, we can better elucidate the nature of the driving forces behind the formation of the static component of the potential difference, as well as the relevant space and time scales for the system.

In the current study of an ITIES system, we use the Nernst−Planck−Poisson equation set (eqs 2.1−2.3) and the same computational set up as in our previous work.[7] As far as the authors are aware, all previous studies elucidating the dynamic theory of three-species potential difference formation were focused on single solvent interfaces.[13,14] We will revise here, in brief, some important methodological aspects.

1.2. Thermodynamic Considerations for ITIES. Consider a salt partitioning between two phases r and l (i.e., right and left), which represent the two immiscible solvents of an ITIES.

Received: May 24, 2011
Revised: September 20, 2011
Published: September 21, 2011

We may define a salt partition coefficient as:

$$K_s = \frac{a_{AB,r}}{a_{AB,l}} \quad (1.1)$$

where $a_{AB,q}$ is the activity of AB in the phase q.

Noting that it is the dissociated ions that will in fact partition between the phases, we have

$$K_i = \frac{a_{i,r}}{a_{i,l}} \quad (1.2)$$

with $i = A^+$ or B^-. K_i is the "single ion partition coefficient" of the ion i.

It follows thermodynamically that the salt partition coefficient and single ion partition coefficients for a binary monovalent salt (or any binary salt of $A^{z+}B^{z-}$ form) are related as[7]

$$K_s = \sqrt{K_+ K_-} \quad (1.3)$$

For a two phase system in equilibrium, the chemical potential μ_q is equivalent for both phases, i.e.,

$$\mu_l = \mu_r \quad (1.4)$$

The chemical potential is a sum of constituent chemical and electrochemical terms, such that

$$\mu_{i,q} = \mu^\circ_{i,q} + RT \ln a_{i,q} + z_i F \phi_q \quad (1.5)$$

where ϕ_q is the potential of phase q, and $\mu^\circ_{i,q}$ is the standard chemical potential.

Using the thermodynamic relationship $\Delta G^\circ = -RT \ln K$, we can derive the appropriate form of the Nernst equation:[7,10]

$$\Delta\phi = \frac{RT}{z_i F}\left(\ln K_i - \ln\left(\frac{a_{i,r}}{a_{i,l}}\right)\right) \quad (1.6)$$

Now, let us consider a two-phase system with more than two ions. Applying bulk electroneutrality to each solution gives

$$\sum_i z_i C_{i,r} = 0 \qquad \sum_i z_i C_{i,l} = 0 \quad (1.7)$$

where $C_{i,q}$ is the concentration of i in phase q. Rearranging eq 1.6 and assuming high dilution ($a_{i,q} \simeq c_{i,q}$),

$$\left(\frac{C_{i,l}}{C_{i,r}}\right) = K_i^{-1} \exp\left(\frac{z_i F}{RT}\Delta\phi\right) \quad (1.8)$$

Substituting eq 1.8 into eq 1.7, and assuming that $c_{i,r} = c_{i,l}$ and that both are equal to a given bulk concentration c^*_i, this gives

$$\sum_i \frac{z_i C^*_i}{1 + \exp\left(\frac{z_i F}{RT}\Delta\phi - \ln K_i\right)} = 0 \quad (1.9)$$

This clearly shows that, at equilibrium, the potential difference between two phases ($\Delta\phi$) is related to the single ion partition coefficients and the amount of individual ions present in both solutions,[10] although not in a way that $\Delta\phi$ can be expressed in closed form, unlike the two-species case.

1.3. Scope of This Work. The current work attempts to expand our previous study of an ITIES system[7] within a common theoretical framework, and therefore an extensive study has been conducted analyzing the effects of single ion partition coefficients, salt partition coefficients, as well as the effect of diffusion coefficients on several aspects of the dynamically evolving system, including the potential difference, the electric field and the ion flux across the ITIES. The water−nitrobenzene system was selected for the study for two reasons: it is the most commonly used system for experimental investigations of a polarized ITIES and has since become a standard for modern investigations;[1,8,15,16] and it is the same system used in our previous work,[7] which allows us to draw direct comparisons between the current work concerning an ITIES with two binary electrolytes with a shared ion and previous work concerning an ITIES with a single binary electrolyte.

Equilibration is simulated for a water−nitrobenzene system for several salts with different salt partition coefficients and diffusion coefficients. Theoretical analysis of the ITIES system and correlation with simulation data is performed, confirming certain classical calculations for the static potential difference for multiple ions,[10] as well as explicitly linking the magnitude of the potential difference to the degree of charge separation throughout the system, and providing a new, more insightful form for the expression of the static component of the potential difference for a two-species system. The presence of static and transient components of the potential difference is confirmed, with the transient component collapsing when the system reaches steady state, thus showing agreement with the modern understanding of the role of diffusional processes in potential difference formation.[7,13,14] We show that potential differences for two electrolytes with a common ion cannot be inferred simply by the addition of single salt potential differences. Moreover, the time scales for formation of the static and diffuse components of the potential difference are revealed, and the significance of diffusion coefficients for not only the magnitude of the diffuse component of the potential difference, but for the dynamic evolution of the system overall, is shown. Finally, observations are made of the more complex behavior displayed during system evolution and comparisons drawn to the simpler system investigated in our previous work.[7] The investigation into the dynamic behavior showed that discussing the dynamic evolution of potential difference across the ITIES and other aspects of the system in terms of three temporal stages is appropriate where these represent partition of ions, transition under the influence of ions,

Table 1. Normalization Relationships and Parameter Definitions

parameter	definition
ϕ	potential
C_i	concentration of species i
z_i	charge of species i
D_i	diffusion coefficient of species i
$C^*_{i,r}$	bulk concentration of a standard species i (RHS)
$D_{i,r}$	the diffusion coefficient of the species i (RHS)
ε_s	dielectric constant of the solvent
ε_0	permittivity of free space
θ	$(F/(RT))\phi$
c_i	$(C_i)/(C^*_{A+,r})$
D'_i	$(D_i)/(D^*_{A+,r})$
X	kx
τ	$k^2 D_{A+,r} t$
k^2	$(F^2 C^*_{A+})/(RT\varepsilon_s\varepsilon_0)$
α	$(\varepsilon_{s,r})/(\varepsilon_{s,l})$
β	$(D'_{i,r})/(D'_{i,l})$

transition under the influence of an electric field, and restoration of electroneutrality, respectively.[7]

2. THEORETICAL MODEL

2.1. Model for an ITIES. For two immiscible solvents with different dielectric constants, consider the formation of a planar interface when the two solvents are brought into contact. In our simulation space, the interface is perpendicular to the linear coordinate x, along which mass transport occurs. We assume that in planes parallel to the plane of the liquid−liquid interface, the solutions are homogeneous, and therefore there is negligible mass transport in all directions save that along the x coordinate. Simulations start at $t = 0$, when the ions are allowed to begin partitioning between the two solvents.

Taking into account the difference in diffusion coefficients of ions in two solvents with different dielectric constants gives the following modified dimensionless Nernst−Planck−Poisson equations[7] (see Table 1 for a list of the definitions and normalization relationships applied):

$$\frac{\partial^2\theta}{\partial X^2} + \sum_i z_i c_i = 0 \tag{2.1}$$

$$\text{RHS}: \quad \frac{\partial^2 c_i}{\partial X^2} - z_i c_i \sum_k z_k c_k + z_i \frac{\partial c_i}{\partial X}\frac{\partial \theta}{\partial X} = \frac{1}{D'_{i,\mathrm{r}}}\frac{\partial c_i}{\partial \tau} \tag{2.2}$$

$$\text{LHS}: \quad \alpha\left(\frac{\partial^2 c_i}{\partial X^2} - z_i c_i \sum_k z_k c_k + z_i \frac{\partial c_i}{\partial X}\frac{\partial \theta}{\partial X}\right) = \beta\left(\frac{1}{D'_{i,\mathrm{r}}}\frac{\partial c_i}{\partial \tau}\right) \tag{2.3}$$

2.2. Boundary Conditions. In order to solve the NPP equation set, appropriate boundary conditions must be applied at the spatial edges of simulation space and at the liquid−liquid interface.

The simulations achieve the effect of limitless bulk solution by making the simulation space pseudoinfinite, i.e., the diffusion layer does not reach the edge of simulation space at any point during the simulation run. This condition is satisfied by setting X_m, which defines the extent of simulation space, to be much greater than the root-mean-square displacement of molecules in time, which is $(2Dt)^{1/2}$, from the Einstein relation:

$$X_{\mathrm{m,r}} = 6\sqrt{D\tau_\mathrm{m}} \quad \text{and} \quad X_{\mathrm{m,l}} = 6\sqrt{D\alpha\tau_\mathrm{m}} \tag{2.4}$$

where D is the largest normalized diffusion coefficient and τ_m is the maximum τ value for the simulation. Thus, we ensure that the diffusion layer does not reach the edge of the simulation space during the simulation. The outer boundary conditions placed upon the concentration of species i are of Dirichlet type, ensuring that material exchange at the outer boundaries does not take place and leads to the simulation space being a Gaussian box of zero enclosed charge. Hence, for all values of τ, $c_{i,q}$ values remain constant,and the electric field (ξ) is zero:

$$X \rightarrow +\infty \quad c_i = c^*_{i,\mathrm{r}} \qquad X \rightarrow -\infty \quad c_i = c^*_{i,\mathrm{l}} \tag{2.5}$$

and

$$X \rightarrow \pm\infty \quad \frac{\partial\theta}{\partial X} = 0 \tag{2.6}$$

where $c^*_{i,q}$ is the bulk concentration for species i in phase q.

A Nernstian condition is applied at the liquid−liquid interface, assuming that the concentrations will be rapidly equilibrated:

$$X = 0 \quad c_{i,\mathrm{l}}K_i = c_{i,\mathrm{r}} \quad \text{with} \quad K_i = \exp\left(\frac{-\Delta G^{\circ,\mathrm{l}\rightarrow\mathrm{r}}_{\mathrm{trs},i}}{RT}\right) \tag{2.7}$$

Note that we assume that the two solvents display ideal immiscibility: the interface between the two solvents is planar and is of negligible thickness. This means that the *potential of mean force* describing the differential stabilization in the two solvents is included in eq 2.7 as localized to the infinitesimally small thickness of the liquid−liquid interface. As has been demonstrated by the experimental study of Luo et al.,[17] the potential of mean force will affect spatial ion concentration profiles within $\leq \pm$ 15 Å of the liquid−liquid junction. However, importantly, under the conditions of the simulation, the spatial extent of this perturbation is not significant and is much smaller than a typical Debye length at low concentration ($x_\mathrm{D} \simeq 10$ nm for a typical concentration of 1 mM). It should not have a significant impact on the dynamic evolution of the system beyond the very immediate vicinity of the liquid−liquid interface, hence ensuring that the approximation for the central boundary condition given by eq 2.7 is valid.

2.3. Numerical Methods. The simulation space is discretized using an expanding space grid. To increase simulation efficiency and decrease simulation time, the space grid is linear from the interface to some user-defined distance, after which it expands exponentially: this insures that a high proportion of data points are localized at the liquid−liquid interface, where gradients are most extreme; this allows to perform simulations in reasonable time for large values of τ which, due to the outer boundary condition linking X_m and τ_m, require a large space grid.

A fully implicit centrally differenced finite difference discretization method is used in the simulations, applying the Newton−Raphson method to iteratively solve the Nernst−Planck−Poisson equation set. Convergence studies were used to establish appropriate parameters. The simulations were programmed in C++ and run on a desktop computer with four Intel Core2 Quad 2.85 GHz processors with 2.00 GB of RAM, with an average runtime of 10 h.

3. RESULTS AND DISCUSSION

The dynamic evolution of potential differences across an ITIES was simulated until some value of τ where fluxes (j_i) for all the constituent species i across the liquid−liquid interface could be considered negligible $(j_i < 10^{-6})$ and when the potential difference $(\Delta\theta)$ was approximately constant.

Three systems of interest were chosen. First, we consider a system with two salts both having $K_{\mathrm{s},i} > 1$, such that one would expect this system to show similar dynamic behavior to a system with just one salt, as for the majority of values of K_+, both anions will partition in the same direction, either with or against the flux of the cation. Second, we consider a system where one salt has $K_{\mathrm{s},1} > 1$ and the other salt has $K_{\mathrm{s},2} < 1$, such that one would expect

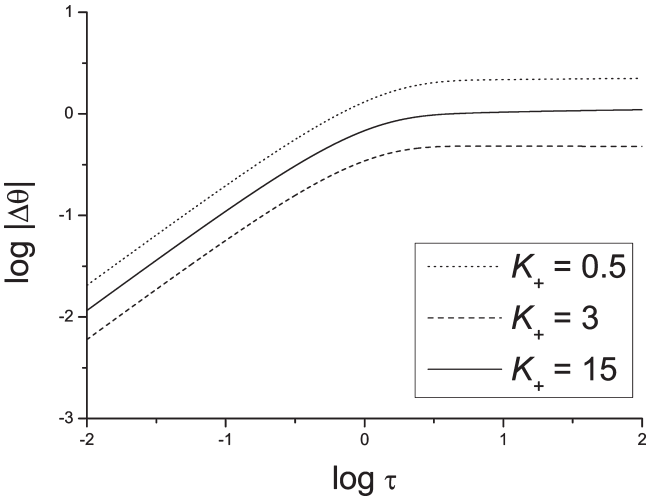

Figure 1. Dynamic evolution of the potential difference, $\Delta\theta$, as a function of time for the partition of the AXY system with $K_{s,1} > K_{s,2} > 1$, for selected values of K_i, on a logarithmic scale.

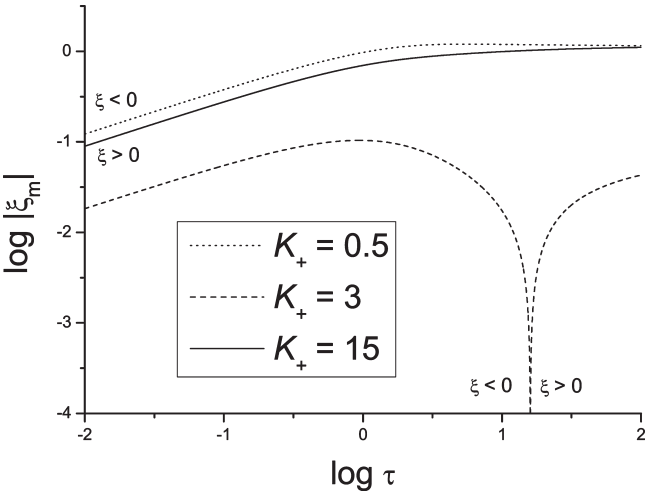

Figure 2. Dynamic evolution of the electric field maximum, ξ_m, as a function of time for the AXY system with $K_{s,1} > K_{s,2} > 1$, for selected values of K_i, on a logarithmic scale.

to see dynamics very different from those of a single binary electrolyte system, under any conditions. Third, we consider a further system of two salts, which was selected as a standard to investigate the effect of changing diffusion coefficients on the dynamics of ITIES potential difference formation.

Appropriately chosen K_s values for the tetra-*n*-butylammonium halide salts, as discussed in our previous investigation of an ITIES with a single electrolyte,[7] fit the required relationships for the K_s values for the systems above. We will use these values, since this will allow us to directly compare the simulation data from this study to our previous investigation of a simpler system. Therefore, certain properties of the TBA^+X^- (where X = Cl^-, Br^-, I^-) salts, such as diffusion coefficients of the constituent ions and K_s values were carried forward for the three-ion systems simulated in the current study.[18−20] Parameters α and β for the water−nitrobenzene system are $\alpha = 2.303$, $\beta \simeq 0.5$.[1]

Specifically, three hypothetical salts AX, AY, and AZ are chosen, which share partition coefficients K_s with TBACl, TBABr, and TBAI as reported in our previous study.[7] The partition coefficients are in the order $K_{sX} > K_{sY} > 1 > K_{sZ}$. The exact values are $K_{sX} = 3.34$; $K_{sY} = 2.20$; $K_{sZ} = 0.305$. The single ion K_i values are varied in order to determine the expected variation of the dynamic behavior of the systems of interest, as a function of these parameters.

3.1. Analysis of Three-Species Systems. *3.1.1. General Considerations.* For the three-ion system in which all the constituent ions partition between the two solutions with different magnitudes and/or different directions, it is expected that in most cases this will lead to permanent charge separation at equilibrium local to the ITIES and hence to a permanent electric field and a static potential difference. Given that charge separation beyond the Debye length is energetically unfavorable, it is expected that any significant charge separation will remain local to the liquid−liquid interface.

Similarly, as ions partition across the ITIES, concentration gradients will form, and given that the ions are likely to have different diffusion coefficients (D_i), the diffusional processes will give rise to charge separation, which will lead to electric field formation and, hence a dynamic potential difference. This is the diffuse component of the potential difference, as the developing electric field will cause migration to occur, which will tend to counter the effects of diffusion by decelerating initially faster species and accelerating initially slower species. As the system tends toward equilibrium, diffusional and migrational fluxes tend toward equal magnitudes, and both tend to zero, with the region of charge separation expanding spatially and decreasing in magnitude throughout the system, thereby maintaining a constant potential difference.[7,13]

However, if the diffusion process is interrupted by an impermeable boundary, the system attains equilibrium in finite time, thereby restoring electroneutrality throughout the system outside the boundary layer. This collapses the diffuse component of the potential difference. If there is a permanent charge separation, then the system will maintain $\Delta\theta \neq 0$, but the transient component will still collapse, so altering the magnitude of $\Delta\theta_{tot}$ of the system. As shown in our previous work,[7] the two components of the potential difference may have the same or opposite signs, depending on the specific values of K_s, K_i, and D_i for the various ions.

3.1.2. $K_{s,1} > K_{s,2} > 1$ Case, AXY System. The AXY system of two salts with $K_{s,1} > K_{s,2} > 1$ partitioning across an ITIES was studied first, in order to determine whether the key features of this more complex system were similar to those of a simpler ITIES model, with only a single salt partitioning. Specifically, the presence and separability of two components for the potential difference was of interest: we expect one component static and local to the ITIES, and one transient and diffuse in nature. Also, we consider the applicability of describing the system dynamics in terms of three temporal stages. The above are key features for a single salt partitioning between two immiscible solvents.[7]

Several key aspects of the equilibrating system were monitored during the simulation, including the dynamic evolutions of the potential difference ($\Delta\theta$), the electric field maximum (ξ_m), the fluxes of all constituent species i at the liquid−liquid interface ($j_{i,X=0}$), as well as spatial profiles for the potential (θ) and concentrations of ions. Additionally, for finite-volume simulations, data for the $c_{i,r}/c_{i,l}$ ratio at the edges of the simulation space were extracted in order to verify that the system approaches Nernstian behavior, as eq 1.6 is attained.

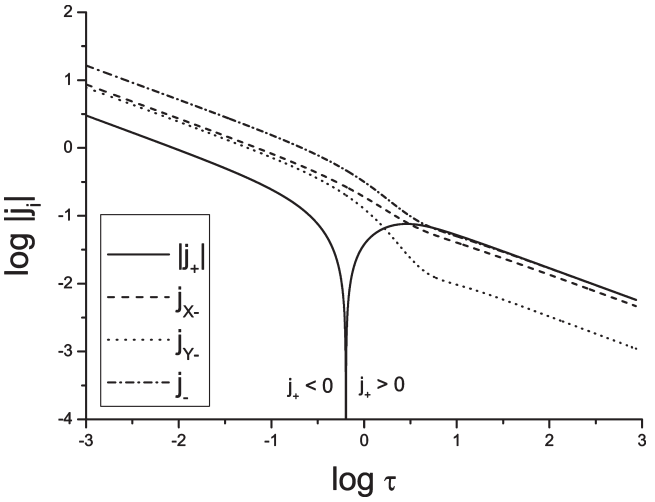

Figure 3. Dynamic evolution of the ionic flux, j_i, as a function of time for the AXY system with $K_{s,1} > K_{s,2} > 1$, assuming $K_+ = 0.5$, on a logarithmic scale.

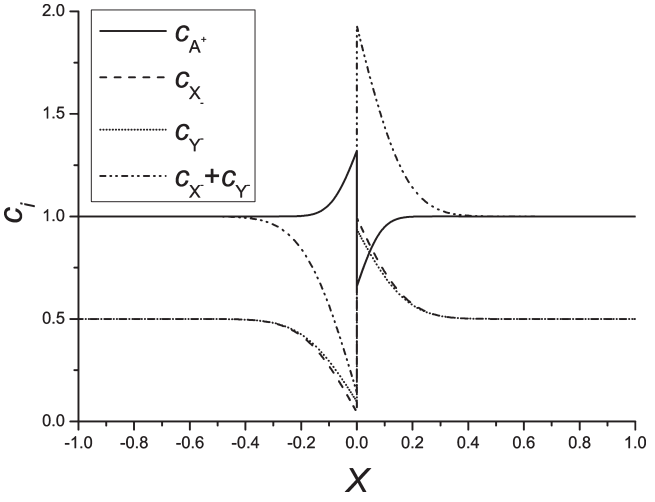

Figure 4. Concentration profiles close to the liquid−liquid interface ($X = 0$) at $\tau = 0.01$ (stage 1) for the AXY system with $K_{s,1} > K_{s,2} > 1$, assuming $K_+ = 0.5$.

Figures 1 and 2 illustrate a typical dynamic evolution of $\Delta\theta$ and ξ_m for this system. Figures 3−5 show typical fluxes across the liquid−liquid junction and concentration profiles at short and long times for the three ions. Figure 6 shows typical electric field profiles at long times.

As can be seen from the aforementioned figures, $\Delta\theta$ and ξ_m demonstrate limiting behavior as $\tau \rightarrow 0$ and $\tau \rightarrow \infty$. Such behavior correlates well with that observed for the partition of a single binary monovalent electrolyte across an ITIES, both qualitatively and with respect to the order of magnitude of τ when there is a qualitative change in the dynamics of evolution of the two system properties. Note that the dynamic evolution of ξ_m for the case of the AXY system where $K_+ = 3$ demonstrates that during the transition from short time to long time behavior there is a change in the sign of ξ_m: this particular dynamic behavior is supported by the electric field profiles for increasing order of magnitudes of τ during the transition stage, and reflects

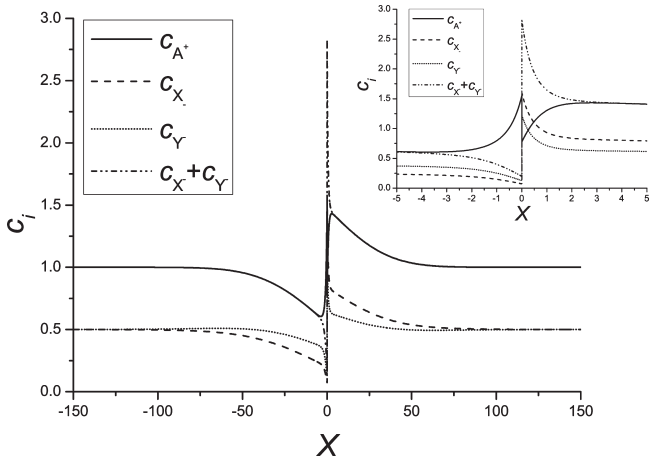

Figure 5. Concentration profiles close to the liquid−liquid interface at $\tau = 10^3$ (stage 3) for the AXY system with $K_{s,1} > K_{s,2} > 1$, assuming $K_+ = 0.5$. Inset: detail of the boundary region.

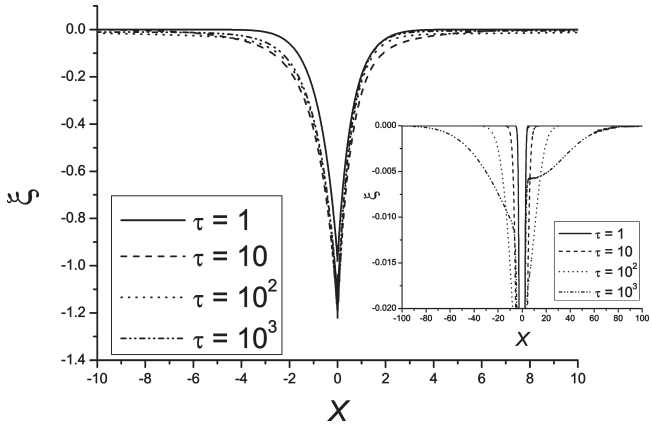

Figure 6. Electric field (ξ) profiles close to the liquid−liquid interface in stages 2 to 3, for the AXY system with $K_{s,1} > K_{s,2} > 1$, assuming $K_+ = 0.5$. Inset: electric field profile in the diffuse component of the potential difference.

the interplay between the two components of the potential difference.

Therefore, we can apply the same descriptive argument as before in correlating the dynamic behavior in Figures 1−5 to three stages: stage 1 is the short time ($\tau \rightarrow 0$) behavior, when the system is dominated by diffusional processes; stage 2 is the intermediate, transitional behavior, when the migration term becomes significant as charge separation from unequal diffusional transport increases; and stage 3 is the long time ($\tau \rightarrow \infty$) behavior, when the migrational and diffusional fluxes tend to vanishingly small and equal magnitudes. The two factors that dominate the system dynamics during stages 1 and 3 are respectively the thermodynamic drive for the ions to partition between the two solutions and attainment of electroneutrality to the maximum degree possible.

The three stages can be temporally and spatially correlated to the Debye length of the system. As can be seen from Figures 4 and 5, the perturbation in the individual anionic concentration profiles expands as $(2\tau)^{1/2}$ in dimensionless form, with the net anionic concentration following a similar pattern. It can be seen that stage 1 behavior occurs when $t < x_D^2/2D$ and the diffusion

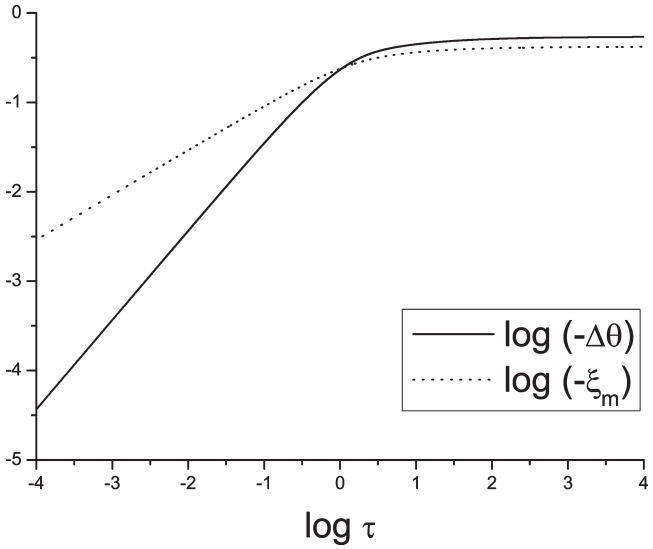

Figure 7. Dynamic evolution of the potential difference, $\Delta\theta$, and electric field maximum, ξ_m, as a function of time for the AYZ system with $K_{s,2} > 1 > K_{s,1}$, assuming $K_+ = 0.5$, on a logarithmic scale.

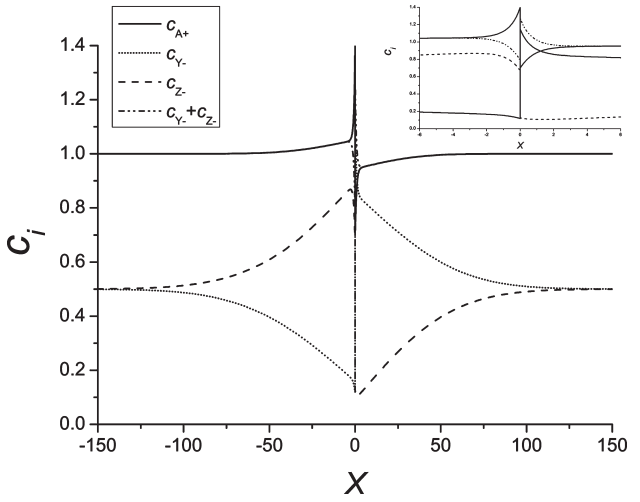

Figure 8. Concentration profiles close to the liquid−liquid interface at $\tau = 10^3$ (stage 3) for the AYZ system with $K_{s,2} > 1 > K_{s,1}$, assuming $K_+ = 0.5$. Inset: detail of the boundary region.

layer is smaller than the Debye length, meaning that charge separation is effectively unconstrained within the region of perturbation, and the behavior is directed by ionic partition. Stage 2 arises when $t \simeq x_D^2/2D$ and the diffusion layer starts to extend beyond the Debye length, which leads to the system starting to restore electroneutrality. Stage 3 occurs when $t > x_D^2/2D$, and most of the diffusion layer is beyond the Debye length, meaning that the system dynamics are dominated by elimination of charge separation in order to fully restore electroneutrality outside the boundary layer.

The discussion above, in terms of increasing and decreasing charge separation, as well as the relative magnitudes of the transport terms, can be illustrated and supported by data such as those in Figure 3, which plots the fluxes (j_+ for the cation, j_- for the anion) of each species with respect to τ on a logarithmic scale. For a two-species case, the picture is relatively simple, as the flux data is extracted at the liquid−liquid junction and initially both solutions are electroneutral: by comparing the direction and magnitude of the two fluxes, it is possible to qualitatively follow the dynamics of the rate of charge separation in the two solvents and, therefore, the minimization of charge separation within the system. For stage 1 behavior, dominated by diffusional processes, we see the faster species, the anion in this case, having greater flux ($j_+ < j_-$), which leads to charge separation. During stage 2, when the system starts to eliminate charge separation within the system, we see flux inversion, such that $j_+ > j_-$, which leads to reduction of charge separation within the system. During stage 3, the reduction in flux magnitude and in magnitude of $|j_+ - j_-|$ displays asymptotic behavior with $j_+ \rightarrow j_- \rightarrow 0$ and $|j_+ - j_-| \rightarrow 0$ as $\tau \rightarrow \infty$, indicating that in the $\tau \rightarrow \infty$ limit, no charge excess will be present in either solution and it is possible to establish complete electroneutrality throughout the solution.

The way in which the system behaves in the transitional period is expected to be more complex for a three species case, since the fluxes of three ions contribute to the transition from the ion-partition-driven behavior in stage 1 to the electroneutrality-driven behavior in stage 3. The sum of the fluxes for the two anions ($j_{X-} + j_{Y-} = j_-$) must tend to j_+ . As Figure 3 demonstrates, for the AXY system with $K_+ = 0.5$, $K_{sX} = 3.34$, $K_{sY} = 2.20$, the anionic fluxes are both in the same direction, with the cationic flux in the opposite direction during stage 1, which leads to increasing charge separation within the system. During stage 2, the cationic flux changes sign and the cations start flowing in the same direction as anions, thereby, reducing the rate of charge separation due to ionic movement within the system. It can be seen that around $\tau = 0.5$, the magnitude of j_+ becomes greater than that of j_- and remains so at long times, although it is worth noting that, as $\tau \rightarrow \infty$, all fluxes tend to zero, as diffusion and migration terms tend to equal magnitude. This indicates that after reaching a certain maximum, charge separation within each solution is reduced at long times, which is in line with the reasoning that the system dynamics are dominated by restoration of electroneutrality outside the boundary layer. It can also be seen from Figure 3 that the restoration of electroneutrality during stage 3 does not *entirely* compensate the charge separation created in stage 1, which is in line with the data showing that there remains a permanent charge separation within the system, even as the potential difference reaches an apparent steady state.

3.1.3. $K_{s,1} > 1 > K_{s,2}$ and $K_{s,2} > 1 > K_{s,1}$ Cases. The other system of significance is that where one salt has $K_s > 1$ and the other has $K_s < 1$, in which the two salts partition in opposite directions. For most normal values of K_+, this implies that both anions partition in opposite directions. As can be seen from Figure 7, the overall behavior for the dynamic evolutions of $\Delta\theta$ and ξ_m is similar, although it is worth noting that in stage 3, the potential difference does not attain its limiting value until longer times than for the AXY system above. Also note that in Figure 8 the diffusion layer is not as pronounced at longer times as in the $K_{s,1} > K_{s,2} > 1$ case, since here the anions partition in opposite directions, so the depletion of one anion in one solution can be compensated by an increase in the concentration of the other anion in the same solution. This leads to a less pronounced perturbation of the cationic species, since the net charge separation is less.

All simulations revealed behavior that could be discussed in terms of the three-stage description of the dynamics, with the general system evolution initially controlled by the values of K_i for each individual ionic species, thus determining the magnitude and direction of the ionic fluxes during stage 1. This then sets up

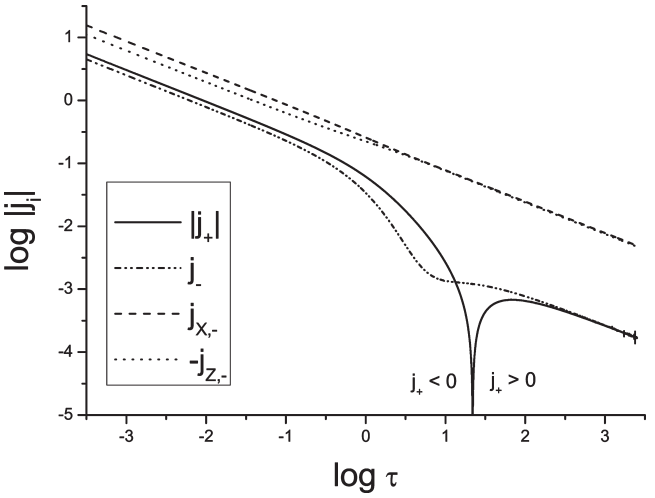

Figure 9. Dynamic evolution of the ionic flux, j_i, as a function of time for the AXZ system with $K_{s,1} > 1 > K_{s,2}$, assuming $K_+ = 0.5$, on a logarithmic scale.

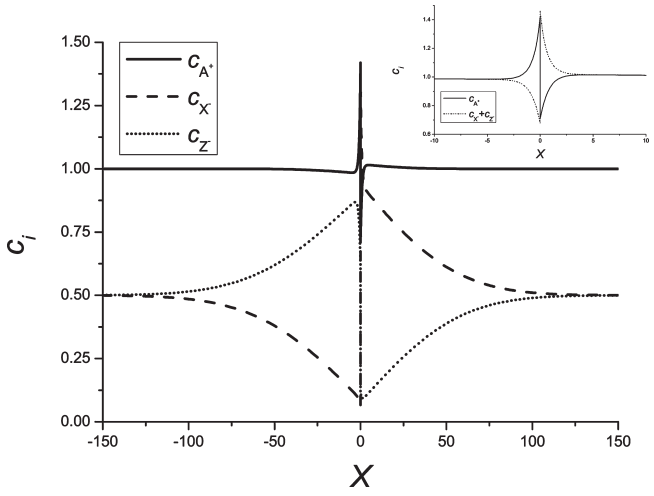

Figure 10. Concentration profiles close to the liquid−liquid interface at $\tau = 10^3$ (stage 3) for the AXZ system with $K_{s,1} > 1 > K_{s,2}$, assuming $K_+ = 0.5$. Inset: detail of the boundary region.

numerous possibilities for the dynamic evolution of fluxes across the liquid−liquid interface during stage 2, as the system adjusts to restore electroneutrality, leading to stage 3 behavior, where only permanent local charge separation is retained as the system tends toward equilibrium. Given that during stage 3, asymptotic behavior is displayed as the migrational and diffusional fluxes tend toward balancing each other out, the dynamic evolution is effectively the same for all cases: the fluxes decrease as $\tau^{-(1/2)}$ with a concomitantly decaying difference in magnitude between j_+ and j_- . Therefore, the greatest variation in behavior occurs during stage 2, although exceptions can be found. The following two examples illustrate the variety of dynamic behavior observed from the simulations, including the case where a change in direction of flux occurs during stage 1.

Figure 9 shows data for the AXZ system, in which the two anions partition in opposite directions, with species X^- having the most extreme K_i value, and therefore a largest flux during stage 1. The cation and species Z^- partition into the same solvent, and hence their fluxes are initially in the same direction. Note that the net anionic flux is opposite to that of the cationic flux and is smaller in magnitude. This leads to a build-up of of excess positive charge in the left solution (nitrobenzene) and excess negative charge in the right (water). As the diffusion layer expands beyond the Debye length and the migration term becomes significant, the fluxes of the anions become closer in magnitude, as can be clearly seen from the steep drop in magnitude of j_-, but a much greater drop in magnitude occurs in j_+. This eventually leads to direction reversal of the cationic flux as stage 3 behavior is approached, where the magnitude of cationic flux tends toward net anionic flux, thereby resulting in a vanishingly small charge separation in either solvent. Note that as the cationic species has the closest K_i value to unity, movement of the cations into a solution with less favorable solubility presents the least energetically costly pathway for the system to restore electroneutrality. Overall, most of the charge separation within the system occurs during stage 1, with a sharp decrease in the amount of charge separation occurring during stage 2 and effectively no extra charge separation produced during stage 3, which results overall in the system having a pair of double layers with excess positive charge on the left-hand side and negative charge on the

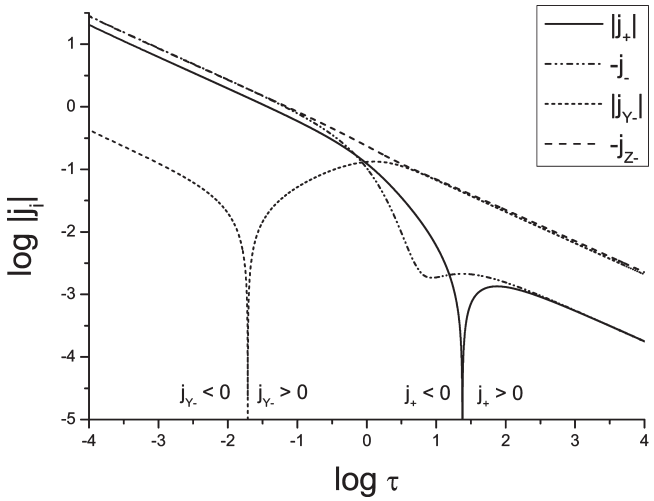

Figure 11. Dynamic evolution of the ionic flux, j_i, as a function of time for the AYZ system with $K_{s,2} > 1 > K_{s,1}$, assuming $K_+ = 5$, on a logarithmic scale.

right-hand side. These conclusions are reflected in the concentration profile of the system at long time ($\tau = 10^4$), as can be seen in Figure 10.

A second example can be seen in Figure 11 for the AYZ system with $K_+ = 5$. Here, due to the more extreme value of K_+, both anions in fact initially partition in the same direction, with the cation partitioning in the opposite direction. This, naturally, leads to significant charge separation in both solvents. However, quite early on, the flux of species Y^- changes direction, reducing the net anionic flux (Figure 11), and hence reducing the rate of charge separation. This can be explained because $K_{Y-} = 0.972$, and so there is very little energetic preference in terms of solvation for species Y^-. Therefore it is more rapidly influenced by the developing electric field. After the charge separation leads to a significant electric field, the flux of the cations is also affected: during stage 2, j_+ changes sign and approaches j_- in the $\tau \rightarrow \infty$ limit. Again, the species

with lower differential preference for solvation tends to the less energetically preferable solvent in order to allow for electroneutrality at long times.

As can be seen from the sections above, an ITIES with three ionic species displays similar key characteristics to an ITIES with two species. Given electric field profiles (e.g., Figure 6), concentration profiles and other dynamic data, the presence of two components of the potential difference, as observed for the case of a single binary salt partitioning across an ITIES,[7] is observed. To verify the transient nature of one of the components, finite volume simulations were set up, such that the diffusion layer encounters an impermeable barrier during the simulation time, thereby ensuring that the system reaches equilibrium in finite time. Simulation data for several cases of K_i values for all systems showed a change in the potential difference of the system when the diffusion layer encounters the spatial boundary, indicating the presence of a transient component of the potential difference, and the resultant equilibrium potential differences were in close agreement with those predicted by classical theory (see eq 1.9).

3.2. Theoretical Treatment of the Three-Species Case. Under the assumption of separability of the two components of the potential difference, theoretical calculations have been performed on each component separately, to further elucidate the nature of the two components in terms of their separability and time scales, and to probe the nature of the relationship between the potential differences for a mixture of salts with a common ion with those for each salt in isolation.

3.2.1. Static Component of the Potential Difference, $\Delta\theta_{stat}$. Consider the Nernst equation (eq 1.6) for the potential difference expressed in terms of behavior of a constituent ion within the system: the dimensionless form of the equation, with assumption of $c_i = a_i$, is given below:

$$\Delta\theta = \frac{1}{z_i}\left(\ln K_i - \ln\left(\frac{c_{i,r}}{c_{i,l}}\right)\right) \tag{3.1}$$

Now, this gives the potential difference at equilibrium, and so provides information only about the magnitude of the static component of the potential difference. For the case of a single binary monovalent electrolyte partitioning across an ITIES, the equation above is transformed to give[7]

$$\Delta\theta = \frac{1}{2}\ln\left(\frac{K_+}{K_-}\right) \tag{3.2}$$

Note that eq 3.2 has been derived by imposing the bulk electroneutrality condition on the system. For a three ion case, the situation is more complex. However, by considering the case where $\Delta\theta = 0$ and the system is fully electroneutral, and applying it to the equation for multiple ions (see eq 1.9), it is possible to solve for a value of K_+, labeled $K_{+,0}$, under which the static component of the potential difference will be zero (see Supporting Information A). The result is a cubic equation, the real root of which gives $K_{+,0}$, which can then be substituted into eq 3.1 for the cation ($K_{+,0} = c_{i,r}/c_{i,l}$) in the same manner as for the two ion case, giving

$$\Delta\theta_{stat} = \ln\left(\frac{K_+}{K_{+,0}}\right) \tag{3.3}$$

with

$$2K_{+,0}^3\left(\frac{1}{K_{s,1}^2K_{s,2}^2}\right) + K_{+,0}^2\left(\frac{1}{K_{s,1}^2} + \frac{1}{K_{s,2}^2}\right) - K_{+,0}\left(\frac{1}{K_{s,1}^2} + \frac{1}{K_{s,2}^2}\right) - 2 = 0 \tag{3.4}$$

Thus, *at equilibrium*, the potential difference can be expressed separably in terms of the single ion partition coefficient of the common ion between the two electrolytes, and a factor $K_{+,0}$, which represents K_+ for the special case where the ions partition in such a way as to not cause permanent charge separation within the system. In this case, charge separation arises only temporarily from diffusional processes and is not retained at equilibrium. Therefore, the magnitude of the static component of the potential difference can be described in terms of the degree of deviation of the system from complete electroneutrality at equilibrium, and therefore this serves as an indication of the degree of permanent charge separation local to the liquid−liquid interface. Finite-volume simulation for several systems with $K_+ = K_{+,0}$ confirmed the eventual collapse of the entire potential difference of the system, when the diffusion layer reaches the boundary of simulation space and so the system reaches a fully electroneutral equilibrium.

Significantly, although $K_{+,0}$ is a function of $K_{s,1}$ and $K_{s,2}$, $K_{+,0} \neq (K_{s,1}K_{s,2})^{1/2}$, as is the case for the two-ion system. This means that the static component of the potential difference is not additive for systems with a common ion, which is to say that the potential difference observed on combining the two salts $A^{z+}X^{z-}$ and $A^{z+}Y^{z-}$ will not be the mean potential difference of the two-ion potentials.

Also note that the equation for the static component of the potential difference for a single monovalent binary electrolyte can be rewritten as

$$\Delta\theta = \frac{1}{2}\ln\left(\frac{K_+}{K_-}\right) = \ln\left(\frac{K_+}{K_s}\right) \tag{3.5}$$

This new formulation of eq 3.2 provides more insight into the nature of the static component of the potential difference, as it also clearly shows the dependence of this component on the degree of deviation from complete electroneutrality throughout the system *at equilibrium*. Note that if $K_+ = K_s$, then, from eq 1.3, $K_+ = K_-$ and, therefore, $\Delta\theta = 0$, and there is no charge separation within the system at equilibrium, as confirmed by prior simulation data.[7]

3.2.2. Transient Component of the Potential Difference, $\Delta\theta_{dyn}$. Asymptotic analysis in the $\tau \rightarrow \infty$ limit was originally used by Hickman and Jackson to analyze the long time behavior of type 1 liquid junctions,[21,22] and was used to derive an expression for the transient, dynamic component of the potential difference for an ITIES with a single binary electrolyte partitioning.[7] Unfortunately, this approach does not yield an analytical solution for a three-species case. Although an expression cannot be obtained analytically, the simulation data for $\Delta\theta_{dyn}$ show clear dependence on the $K_{+,0}$ and D_i values, indicating a more complicated relationship (Figure 12) than for the case of a single binary electrolyte partitioning between

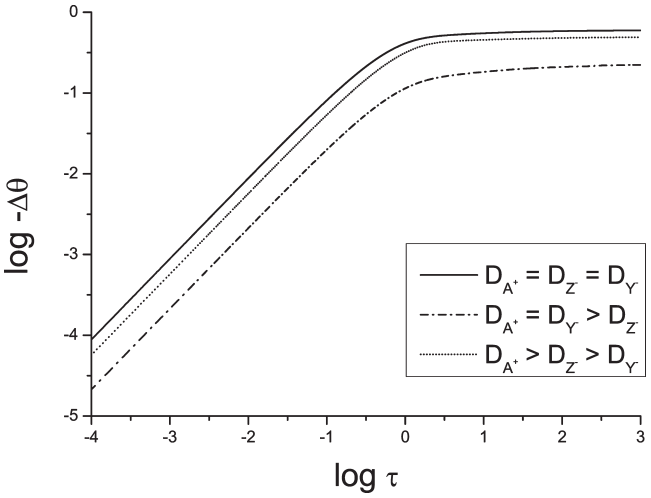

Figure 12. Dynamic evolution of the potential difference, $\Delta\theta$, as a function of time for the AYZ system with $K_{s,2} > 1 > K_{s,1}$ and $K_+ = 0.5$, for selected values of D_i, on a logarithmic scale.

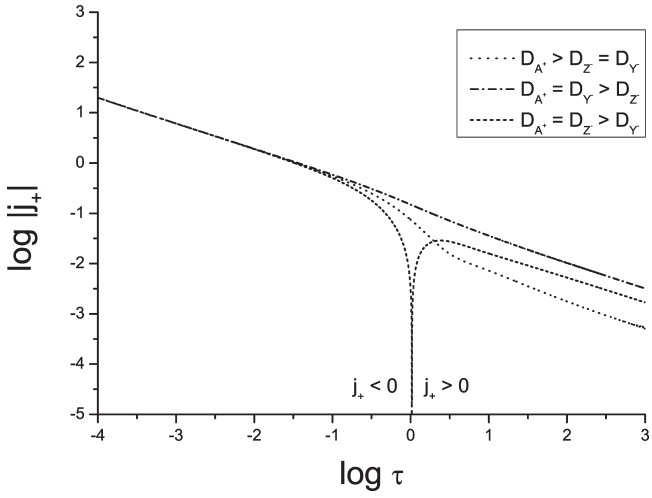

Figure 13. Dynamic evolution of the cationic flux, j_+, as a function of time for the AYZ system with $K_{s,2} > 1 > K_{s,1}$ and $K_+ = 0.5$, for selected values of D_i, on a logarithmic scale.

two immiscible solutions, where $\Delta\theta_{dyn}$ has the following expression:[7]

$$\Delta\theta_{dyn} = \delta \ln K_s \qquad \delta = \frac{(D_+ - D_-)}{(D_+ + D_-)} \qquad (3.6)$$

However, we note that the situation where $D_{1-} \simeq D_{2-}$ is not infrequent, e.g., the difference in diffusion coefficients of the chloride, iodide, and bromide ions in water is less than 2%,[19] and electrolytes with these anions, or other similar electrolytes, are commonly encountered,[8,15,16,20] therefore $D_{1-} = D_{2-} = D_-$ could be a useful and reasonable approximation for some three-ion systems.

We also note that for the three-ion system, $K_{+,0}$ from eq 3.3 is fundamentally similar to K_s from eq 3.5: in both cases, this is the value of K_+ under which, at equilibrium, the system can attain complete electroneutrality and, for the three species case, this is where the partition of the cationic species across the ITIES and the net effect from partition of the two anionic species will be the same in both magnitude and direction, meaning no permanent charge separation remains at equilibrium. It is worth noting that $K_{+,0}$ serves as $K_{s,app}$ for the system and is independent of K_i or D_i, as can be seen from eqs 3.3 and 3.5. This is supported by data from simulations that show that in all cases, for any combination of K_i and D_i values for a given set of $K_{s,1}$ and $K_{s,2}$, outside the boundary layer, $c_{+,r}/c_{+,l} \rightarrow c_{-,r}/c_{-,l} \rightarrow K_{+,0}$, as $\tau \rightarrow \infty$, as required by the Nernst equation. Hence, we can define $K_{-,app} \equiv K_{+,0} \simeq c_{-,r}/c_{-,l}$, where $c_- = c_{1-} + c_{2-}$ (see Figures 5, 8, and 10). Thus, although it is not possible to quantitatively predict the behavior of individual anionic species, it is possible to do so for the net anionic concentration.

Therefore, by taking an three-ion system where $D_{1-} = D_{2-} = D_-$, and applying the above considerations, the problem becomes mathematically equivalent to the two species case since, to maintain electroneutrality outside the boundary layer, the combination of the two anions acts as a single anion with a corresponding apparent single salt partition coefficient $K_{s,app}$ equaling $K_{+,0}$. Substituting into eq 3.6, the following expression for $\Delta\theta_{dyn}$ is obtained (mathematical details are given in Supporting Information B):

$$\Delta\theta_{dyn} = \delta \ln K_{+,0} \quad \delta = \frac{(D_+ - D_-)}{(D_+ + D_-)} \qquad (3.7)$$

To verify the validity of this expression, two simulations with anions having equal diffusion coefficients were run; the total potential difference of the system, calculated from the sum of eqs 3.3 and 3.7, was within 4.5% of $\Delta\theta_{simulation}$ for $\tau = 10^4$.

Thus, although an expression cannot be obtained for a general three-ion case, and it is not possible to quantitatively predict the concentration profile of individual anionic species; for the case where $D_{1-} \simeq D_{2-}$, it is nevertheless possible to predict $\Delta\theta_{dyn}$ to reasonable accuracy and to associate the general behavior of the net anionic concentration with the cation concentration profile, in accordance with electroneutrality. As with the static potential difference, the constant $K_{+,0}$ is understood to act as an apparent K_s for the multispecies system.

3.3. Investigating the Effect of D_i on System Dynamics. Up to this point, the investigation of the dynamics of potential differences across an ITIES has been focused on the effect of the K_i values of each individual ion, with all systems using the D_i values for the set of TBA^+X^- (where $X^- = Cl^-$, Br^-, I^-) salts, and with the halides having roughly the same diffusion coefficients. This resulted in all cases having a cation diffusing at a rate roughly 4 times slower than the anions. However, as can clearly be seen from eq 3.6, diffusion coefficients play a key role in determining the overall potential difference of an equilibrating system. The AYZ case with $K_+ = 0.5$ was chosen as a standard system, and several different sets of relative D_i values were investigated. This particular system was chosen to provide disparate magnitudes of partition of the individual ionic species, and also since it exhibits typical flux evolution dynamics and gives fast simulation runtime under standard conditions.

Logic dictates that diffusion coefficients will have a significant impact on the dynamics of the system evolution, as the potential difference results initially from distinct diffusion coefficients of the three species. This is supported by the interesting internal dynamics observed for these simulations, such as those in Figure 13, where the effect of changing the ratios of the diffusion coefficients of the three species leads to the dynamic evolution of

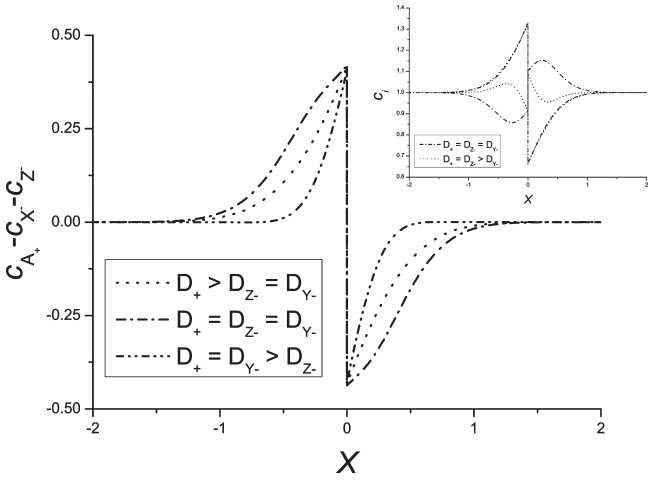

Figure 14. Charge separation profiles close to the liquid−liquid interface at $\tau = 0.01$ (stage 1) for the AYZ system with $K_{s,2} > 1 > K_{s,1}$ and $K_+ = 0.5$, for selected values of D_i.

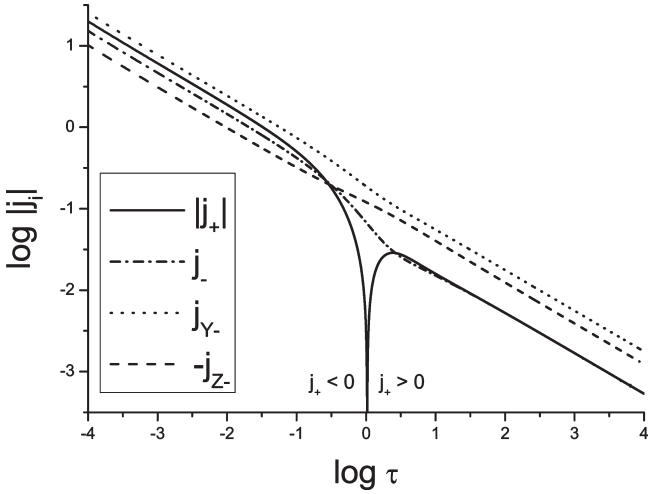

Figure 15. Dynamic evolution of the ionic flux, j_i, as a function of time for the AYZ system with $K_{s,2} > 1 > K_{s,1}$ and $K_+ = 0.5$, for the case of $D_+ = D_{2-} > D_{1-}$, on a logarithmic scale.

the flux for the cation, j_+, varying greatly during the transitional stage 2, and results in j_+ varying across 1 order of magnitude during stage 3.

Note that in all cases, the short-term behavior is similar: this is the time when the evolution of the system is driven solely by diffusional processes and the diffusion layer is smaller than the Debye length, meaning that charge separation is effectively unconstrained within the diffusion layer and arises from the difference in rates of diffusion of constituent ions. Given that under different conditions, a different degree of charge separation occurs throughout the system at short times (Figure 14), when the system tends to restore electroneutrality outside the boundary layer, the amount of charge separation to be eliminated depends on the dynamics of stages 1 and 2. This results in similar trends, i.e., fluxes decreasing as $\tau^{1/2}$, but with different absolute magnitudes (see Figure 13), such that, as $\tau \rightarrow \infty$, charge separation tends to zero outside the boundary layer.

The change of direction of flow of the cation in stage 2, seen in Figures 13 and 15 for the $D_+ = D_{Y-} > D_{Z-}$ case, can be explained

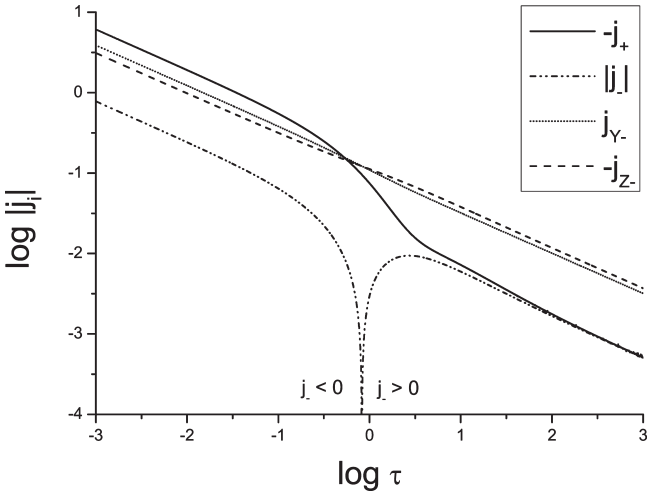

Figure 16. Dynamic evolution of the ionic flux, j_i, as a function of time for the AYZ system with $K_{s,2} > 1 > K_{s,1}$ and $K_+ = 0.5$, for the case of $D_+ > D_{2-} = D_{1-}$, on a logarithmic scale.

in terms of the significance of the relative diffusion coefficients for "selection" of the species that must undergo a change of flux direction to restore electroneutrality. For the particular case highlighted, the initial flux direction is the same for the cation and the second anionic species, but with the net anionic flux in the opposite direction. During the transition stage, when the system moves from unconstrained ionic partitioning across the ITIES to restoration of electroneutrality in the system, the required elimination of charge separation in each solvent leads to the fastest species, with the smallest differential energies for solvation, to respond most quickly and change its direction of flow back toward the solution with poorer solvation, thereby reducing significantly and eventually inverting the rate of charge separation in each solution.

Note that, as demonstrated in the example below, the relative flux magnitudes of individual species and the net anionic flux also play a significant role in determining the dynamics of stage 2. Moreover, it is expected that these factors will have a major impact in cases when the species with the lowest K_i might not have the largest D_i.

Note that in some other cases it is the net anionic flux that changes direction, such as the case $D_+ > D_{Z-} = D_{Y-}$ (Figure 16), where the fluxes for the two anionic species are similar in magnitude, but in opposite directions, with the net anionic flux occurring in the opposite direction to the cationic flux. During stage 2, although the magnitude of the cationic flux begins to reduce significantly in order to decrease the rate of charge separation, the two slower anionic species interchange their flux magnitudes, thereby effectively changing the direction of the net anionic flux to that of the cationic flux, and further reducing the rate of charge separation, *before* the flux of the faster cationic species changes direction. This obviates the need for j_+ to change direction, such that by stage 3 all species continue partitioning in the same direction, but the charge separation within the system is drastically reduced.

Therefore, it is clear that both the single ion partition coefficients and the diffusion coefficients can have a significant impact on the dynamic evolution of the system, with the initial ion partitioning providing the initial direction of fluxes, and with both K_i and D_i values having an impact on the magnitude of the

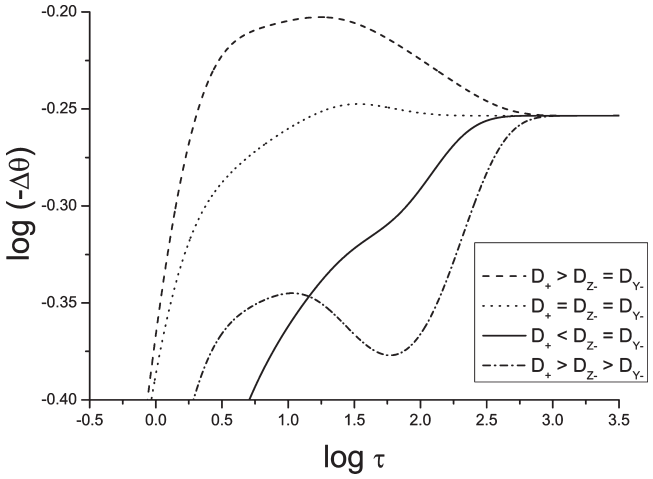

Figure 17. Dynamic evolution of the potential difference, $\Delta\theta$, as a function of time for the AYZ system with $K_{s,2} > 1 > K_{s,1}$ and $K_+ = 0.5$, with solutions of finite volume, for selected values of D_i, on a logarithmic scale. Note that despite the variation of relationships between D_i, the transient component of $\Delta\theta_{tot}$ collapses to the same value of $\Delta\theta_{stat}$, as predicted by theory.

flux of species i during stage 1. The dynamics of transition through stage 2 to stage 3 determine the relative magnitudes of the fluxes of all constituent species: for example, the presence or absence of a crossover point in direction for cationic flux or net anionic flux. These further depend on the extent to which the system will deviate from complete electroneutrality at equilibrium, as determined by the K_i values. The magnitudes of the fluxes are governed by the relative D_i values, indicating the degree of temporary charge separation, which forms the basis of the transient component of the potential difference of the system. The restoration of electroneutrality may affect the flux magnitude and direction, depending on how fast each individual species diffuses in relation to the others, and the magnitude of the energetic differences for the various species in each solution.

3.4. Determining Time Scales for $\Delta\theta_{stat}$ and $\Delta\theta_{dyn}$. One final note should be given on the elucidation of the time scales of $\Delta\theta_{stat}$ and $\Delta\theta_{dyn}$ formation. First, simulations were run with varying D_i values, both for finite and infinite solution volumes (Figure 17). The data clearly show that the transient component duly collapses to the same $\Delta\theta$ value for a given X_m, indicating that this value is independent of D_i and the transient component. Note that, as with the two-species case, the static component of the potential difference has a $|X_m| < 10$ dependence in that only over that space is significant charge separation supported, and that defines the spatial extent of the static component of the potential difference. Beyond the $X \simeq 10$ limit, the difference in $\Delta\theta_{stat}$ is relatively minor (between 0.1%−2% for different systems). Therefore, finite-volume simulations with $|X_m| = 10$ show that that all systems effectively reach the magnitude of $\Delta\theta_{stat}$ predicted from eq 3.3 by $\tau \simeq 100$.

For the transient component of the potential difference, the time scales for the different D_i relationships were inferred from the degree of deviation of $c_{+,r}/c_{+,l}$ from the Nernst equation (eq 3.1), which predicts $K_{+,0} = c_{+,r}/c_{+,l} = K_{s,1}^2(c_{1-,r}/c_{1-,l}) = K_{s,2}^2(c_{2-,l}/c_{2-,r})$ at equilibrium. Data were recorded at $\tau = 10^3$, when the system displays stage 3, and at $|X_m| = 10$, i.e., just outside the spatial extent of perturbations due to the localized static component. The results show that the fastest relative dynamics were for the system where all the D_i values were different (deviation from $K_{+,0} \simeq 1.3\%$), followed closely by cases where all D_i values were the same and those where the anions had the same D_i value (between 4%−5%). The cases with greatest deviation from $K_{+,0}$ were those where the D_+ value was equal to one of the D_i values for the anions, with the other anion being slower (difference between 6% and 15%). This suggests that the systems with fast relative dynamics are those in which the relations between the D_i values lower the initial magnitude of charge separation, such as where all D_i are the same, or are more flexibile in rapidly reducing charge separation or reducing the amount of charge separation within the system, such as where all D_i are different. The systems with the slower relative dynamics had conditions under which electroneutrality takes longer to recover. Further results for different cases are given in Supporting Information C.

Overall, the data indicate that the relative time scales of the formation of the transient component of the potential difference can vary by over an order of magnitude, depending on the fundamental relations between diffusion coefficients.

4. CONCLUSIONS

Detailed dynamic analysis was performed on an ITIES with two different monovalent binary electrolytes, sharing a common cation, initially present in equimolar concentrations in both solvents. The magnitude of the static liquid−liquid potential difference was analytically correlated to an energetic minimum. The dynamic evolution of ionic current across the interface was further investigated, with focus on the net and individual ion fluxes across the ITIES, which displays complex behavior. Time scales for the formation of the static and diffuse components of the potential difference were investigated and correlated with ion partitioning and diffusion effects. It was found that the discussion of the dynamic development of the potential difference and other aspects of the system in terms of three temporal stages was still appropriate, detailed by the relative role of the diffusion layer compared to the Debye length.

An expression for the static potential difference component has been derived and compared to that for an ITIES with a single monovalent binary electrolyte. It was shown that the static component of the potential difference is a separable function of the single ion partition coefficient of the common ion and some function of the partition coefficients of the two salts, and that for systems with a common ion, the single ion potential differences are not additive in nature.

It was shown that the relative magnitudes of the diffusion coefficients can significantly alter the dynamic evolution of the system: for example, under certain conditions, the flux of the cation across the ITIES can switch sign, whereas in most cases the cation flows only in one direction.

Overall, it was shown that a three-species ITIES system shares fundamental aspects of its dynamics with a two-species ITIES system, including the causes of the two components of the potential difference and their dynamics, but displays greater variety and more complex dynamics as the system proceeds from short-time, partition-dominated behavior, to long-time, electroneutrality-dominated behavior. The same general conclusions may likely be extrapolated to any Nernstian ITIES system.

■ ASSOCIATED CONTENT

Supporting Information. (A) Mathematical derivation of the required equation satisfied by $K_{+,0}$; (B) mathematical detail of asymptotic analysis as $\tau \rightarrow \infty$ subject to equivalent diffusion coefficients; (C) simulation data concerning the relative effects of diffusion coefficient ratio upon system dynamics. This information is available free of charge via the Internet at http://pubs.acs.org.

■ AUTHOR INFORMATION

Corresponding Author
*Fax: +44 (0) 1865 275410. Tel: +44 (0) 1865 275413. E-mail: richard.compton@chem.ox.ac.uk.

■ ACKNOWLEDGMENT

E.J.F.D. thanks St. John's College, Oxford, for funding.

■ REFERENCES

(1) Samec, Z. *Pure Appl. Chem.* **2004**, *76*, 2147–2180.
(2) Vanýsek, P.; Ramírez, L. *J. Chil. Chem. Soc.* **2008**, *53*, 1455–1463.
(3) Kivlehan, F.; Lanyon, Y. H.; Arrigan, D. W. M. *Langmuir* **2008**, *24*, 9876–9882.
(4) Watarai, H. *Solvent Extr. Liq. Membr.* **2008**, 21–57.
(5) Ishimatsu, R.; Kim, J.; Jing, P.; Streimer, C. C.; Fang, D. Z.; Fauchet, P. M.; McGrath, J. L.; Amemiya, S. *Anal. Chem.* **2010**, *82*, 7127–7134.
(6) Stockmann, T. J.; Ding, Z. *J. Electroanal. Chem.* **2010**, *649*, 23–31.
(7) Zhurov, K.; Dickinson, E. J. F.; Compton, R. G. *J. Phys. Chem. B* **2011**, *115*, 6909–6921.
(8) Gavach, C.; Savajols, A. *Electrochim. Acta* **1974**, *19*, 575–581.
(9) Koryta, J.; Vanýsek, P.; Březina, M. *J. Electroanal. Chem.* **1977**, *75*, 211–228.
(10) Hung, L. *J. Electroanal. Chem.* **1980**, *115*, 159–174.
(11) Samec, Z. *Chem. Rev.* **1988**, *88*, 617–32.
(12) Kakiuchi, T. *Anal. Chem.* **1996**, *68*, 3658–3664.
(13) Dickinson, E. J. F.; Freitag, L.; Compton, R. G. *J. Phys. Chem. B* **2010**, *114*, 187–197.
(14) Ward, K. R.; Dickinson, E. J. F.; Compton, R. G. *J. Phys. Chem. B* **2010**, *114*, 4521–4528.
(15) Danil de Namor, A. F.; Hill, T.; Sigstad, E. *J. Chem. Soc., Faraday Trans. 1* **1983**, *79*, 2713–2722.
(16) Koczorowski, Z.; Geblewicz, G. *J. Electroanal. Chem.* **1983**, *152*, 55–66.
(17) Luo, G.; Malkova, S.; Yoon, J.; Schultz, D. G.; Lin, B.; Meron, M.; Benjamin, I.; Vanýsek, P.; Schlossman, M. L. *Science* **2006**, *311*, 216–218.
(18) Koczorowski, Z.; Geblewicz, G. *J. Electroanal. Chem.* **1980**, *108*, 117–120.
(19) Bard, A. J.; Faulkner, L. R. *Electrochemical Methods: Fundamentals and Applications*; John Wiley & Sons: New York, 2001.
(20) Markin, V.; Volkov, A.; Volkova-Gugeshashvili, M. *J. Phys. Chem. B* **2005**, *109*, 16444–16454.
(21) Hickman, H. J. *Chem. Eng. Sci.* **1970**, *25*, 381–398.
(22) Jackson, J. L. *J. Phys. Chem.* **1974**, *78*, 2060–2064.